Hindawi Publishing Corporation
Journal of Chemistry
Volume 2013, Article ID 935646, 9 pages
http://dx.doi.org/10.1155/2013/935646

Research Article

2-[3,5-Bis-(2-fluorobenzylidene)-4-piperidon-1-yl]-N-(4-fluorobenzyl)-acetamide and Its Evaluation as an Anticancer Agent

Pallavi Lagisetty, Hrushikesh Agashe, and Vibhudutta Awasthi

Department of Pharmaceutical Sciences and Research Imaging Facility, University of Oklahoma Health Science Center, 1110 N. Stonewall Avenue, Oklahoma City, OK 73117, USA

Correspondence should be addressed to Vibhudutta Awasthi; vawasthi@ouhsc.edu

Received 2 May 2013; Accepted 1 July 2013

Academic Editor: Liviu Mitu

Synthesis of 2-[3,5-bis-(2-fluorobenzylidene)-4-piperidon-1-yl]-N-(4-fluorobenzyl)-acetamide, a derivative of 3,5-bis-(2-fluorobenzylidene)-4-piperidone (EF24), as an antiproliferative and imageable compound is described. The radioactive derivative was synthesized in 40–45% radiochemical yield using N-[4-fluoro(^{18}F)benzyl]-2-bromoacetamide (NFLOBA) as a radiolabeled synthon for coupling with EF24. Cell proliferation assays showed that 2-[3,5-bis-(2-fluorobenzylidene)-4-piperidon-1-yl]-N-(4-fluorobenzyl)-acetamide (NFLOBA-EF24) had antiproliferative efficacy similar to that of EF24 in lung adenocarcinoma H441 cells. ^{18}F-NFLOBA-EF24 was investigated in normal rats for whole-body PET imaging and biodistribution. At necropsy after 1 h of injection, about 12% of injected compound was still circulating in blood; liver, kidney, and muscle were other tissues with moderate amounts of accumulation. In order to assess the tumor-suppressive activity, nonradioactive NFLOBA-EF24 was administered in nude rats carrying xenograft H441 tumor. After 15 days of treatment, the tumor size decreased by approximately 83% compared to the tumors in control rats. The tumor regression was also confirmed by molecular imaging of glucose metabolism with ^{18}F-fluorodeoxyglucose. The results suggest that EF24 could be efficiently modified with ^{18}F-labeled synthon NFLOBA for convenient PET imaging without altering the antitumor efficacy of the original compound. This study provides visual kinetics of synthetic curcuminoid EF24 by positron emission tomography for the first time.

1. Introduction

The importance of imaging in cancer drug development is increasing with advances in instrumentation, chemistry, and imaging technologies [1]. The development of potent and molecularly targeted therapies of cancer could immensely benefit from visual, temporal, and quantitative information pertaining to the delivery of drug in tumor tissue and its clearance kinetics from nontarget tissues. In most instances, molecular imaging technologies are able to provide real-time biodisposition of drugs. Positron emission tomography (PET), magnetic resonance imaging, single photon emission tomography (SPECT), and optical devices are such available technologies in both preclinical as well as clinical settings. Imaging provides both structural and functional information under physiologic conditions and eliminates the sampling errors inherent in other methods [2]. It is also possible to perform longitudinal studies in the same subject to collect time point-specific data. It is not surprising therefore that the role of such technologies in hastening anti-cancer drug development is acknowledged in a Critical Path Initiative by the FDA and NCI [3–5]. Noninvasive imaging enables strategic monitoring of the adequacy and selectivity of drug accumulation in pathologic tissue. For example, in the treatment of non-Hodgkin's lymphoma with ^{90}Y-labeled ibritumomab (Zevalin), the information derived from SPECT imaging of ^{111}In-labeled ibritumomab distribution before initiating radioimmunotherapy is a clinical reality [6].

The objective of the research presented in this article was to use highly sensitive PET imaging technology to monitor real-time disposition of anticancer and anti-inflammatory drugs of synthetic curcuminoid class. Because of low systemic absorption of curcumin, chemically modified chalcone derivatives are being developed as its more

bioavailable compounds [7]. These synthetic curcuminoids are purported to have enhanced biological activity and improved physicochemical properties [8–10]. EF24, 3,5-bis-(2-fluorobenzylidene)-4-piperidone (Figure 1(a)) is the lead compound displaying potent anti-inflammatory and anti-cancer activity both *in vitro* as well as *in vivo* [10–13]. Like curcumin, the exact mechanism of action of EF24 is unclear, but it appears to suppress inflammatory pathway and angiogenesis by downregulating various cancer-promoting genes such as COX-2, IL-8, and VEGF [11]. It has also been found to induce G2/M cell cycle arrest and apoptosis in cisplatin-resistant human cancer cells [12]. A recent study suggests that the antiproliferative activity of EF24 may be related to the suppression of NF-κB signaling by direct inhibition of I-κB kinase [14].

In order to enable investigation of real-time biodisposition of EF24, we report the synthesis of an ^{18}F-labeled EF24 and demonstrate that the modified compound retains antiproliferative activity of the precursor compound in cancer cells. Earlier we have shown that certain modifications at piperidinyl nitrogen of EF24 molecule do not adversely affect antiproliferative activity of EF24 [15]. To our knowledge, this is the first study on PET imaging of 3,5-bis (benzylidene)-4-piperidone. The results enhance our understanding of the kinetics of ^{18}F-labeled EF24 during the early phase of elimination from the body.

2. Experimental Procedures

All reagents were obtained from commercial sources and were used directly without further purification. The synthesis of 2 was accomplished by acid-catalyzed Claisen-Schmidt condensation of 4-piperidone and 2-fluorobenzaldehyde and has been reported elsewhere [13, 16]. ^{1}H NMR spectra and ^{13}C NMR spectra were recorded at 300 MHz and 75 MHz on Varian VX-300 (Varian Inc., CA). The spectra were referenced to the residual protonated solvents. Abbreviations *s*, *d*, *t*, *m*, *br*, and *dd*, used in the description of NMR spectra, denote *singlet*, *doublet*, *triplet*, *multiplet*, *broad*, and *double doublet*, respectively. The chemical shifts and coupling constants were reported in δ parts per million (ppm) and hertz (Hz), respectively. The mass spectra were recorded by Finnigan MAT LCQ mass spectrometer (San Jose, CA). The NMR and mass spectroscopy data are reported in the supplementary material available online at http://dx.doi.org/10.1155/2013/935646.

The reverse phase high-performance liquid chromatography (RP-HPLC) was performed with Knaur system equipped with K1001 HPLC pump, BG-14 degasser, Dynamax UV-1 absorbance detector, Beckman model 170 radioisotope detector, and Peak simple chromatography data acquisition system (SRI, Inc. CA). No-carrier-added fluoride-18 ($^{18}F^-$) ion was obtained from IBA Molecular (Dallas, TX). All the intermediates and final products were monitored by thin layer chromatography (TLC) on 250 μm silica plates. Where applicable, the compounds were purified by column chromatography using 200–300 mesh silica gel columns. The melting points were recorded on an Electrothermal Mel-Temp melting point apparatus (Thermo Scientific, Waltham, MA). The reported melting points (°C) are uncorrected.

2.1. Synthesis of NFLOBA-EF24

*2.1.1. 4-Cyano-N,N,N-trimethylanilinium trifluoromethanesulfonate (**4**).* Methyl trifluoromethanesulfonate (1.13 mL, 9.98 mmol) was added to a solution of 4-(dimethylamino) benzonitrile (**3**, 1.05 gm, 7.18 mmol) in benzene (14 mL). The reaction mixture was heated at 80°C for 1 h under nitrogen atmosphere. The yellow crystalline solid was separated from the reaction mixture on a Buchner funnel and washed with benzene (20 mL). Compound **4** was obtained with 86% yield (1.91 gm, m.p. 144-145°C); R_f (50 : 50 Methanol : Chloroform) = 0.50.

*2.1.2. N-(4-Fluorobenzyl)-2-bromoacetamide (**11**).* Bromoacetyl bromide (380 μL, 4.35 mmol) and triethylamine (600 μL, 4.39 mmol) were added to an ice-cold solution of 4-fluorobenzylamine (**10**, 500 mg, 3.99 mmol) in methylene chloride. The reaction mixture was stirred at room temperature for 20 min. The progress of this reaction was monitored by a faster moving spot of the desired compound on silica TLC (60% ethyl acetate in hexanes). After the reaction was complete, the reaction mixture was filtered, and the filtrate was dried to obtain 2-bromo-*N*-[4-fluorobenzyl]-acetamide (**11**) as a white solid (894 mg, 96% yield, m.p. 93–95°C).

*2.1.3. 2-[3,5-Bis-(2-fluorobenzylidene)-4-piperidin-1-yl]-N-(4-fluorobenzyl)-acetamide (**12**).* Potassium iodide (199 mg, 1.2 mmol), Cs_2CO_3 (325 mg, 1 mmol), and *N*-(4-fluorobenzyl)-2-bromoacetamide (**11**, 270 mg, 1.20 mmol) were added to compound **2** (311 mg, 1 mmol) in DMF (2 mL). The reaction mixture was heated at 85°C for 30 min, before evaporating to dryness and dissolving the residue in chloroform. The organic layer was washed with saturated sodium chloride and subsequently with water. The organic phase was separated, dried over anhydrous sodium sulfate, and concentrated to obtain a crude yellow solid. The crude compound was recrystallized from chloroform and hexanes to obtain the title compound **12** as a yellow crystalline solid (252 mg, 53% yield, m.p. 115–117°C).

2.2. Radiofluorination

*2.2.1. 4-Fluoro[^{18}F]-benzonitrile (**6**).* Kryptofix was dissolved (9 mg, 24 μmol) in 0.5 mL of acetonitrile in a reaction vial. K_2CO_3 (1 mg, 7 μmol) was added to the kryptofix solution in water (15 μL). Radioactivity (^{18}F in water) was added to the vial, and the mixture was heated at 110°C under nitrogen to azeotropically evaporate water. The acetonitrile-driven drying was repeated two more times. The quaternary ammonium triflate salt **4** (5 mg) was dissolved in 250 μL dimethylsulfoxide (DMSO) and added to the kryptofix-^{18}F complex. The reaction mixture was heated at 130°C for 10 min before allowing it to cool down to room temperature. The mixture was diluted with 2 mL water and passed through Sep-Pak Silica and SCX cartridges connected in series. Compound **6** was eluted with anhydrous THF (6 mL) and dried to about 1 mL volume. The ^{18}F-labeled compound **9** was eluted at 15.0 min in radio-UV-RPHPLC (5% to 100%

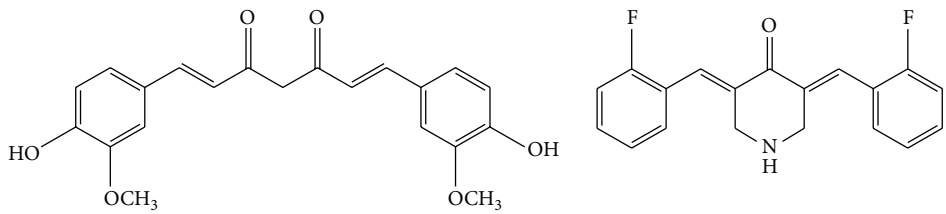

Curcumin (**1**) Diphenyldifluoroketone EF24 (**2**)

Figure 1: Structural features of curcumin and its synthetic analog EF24.

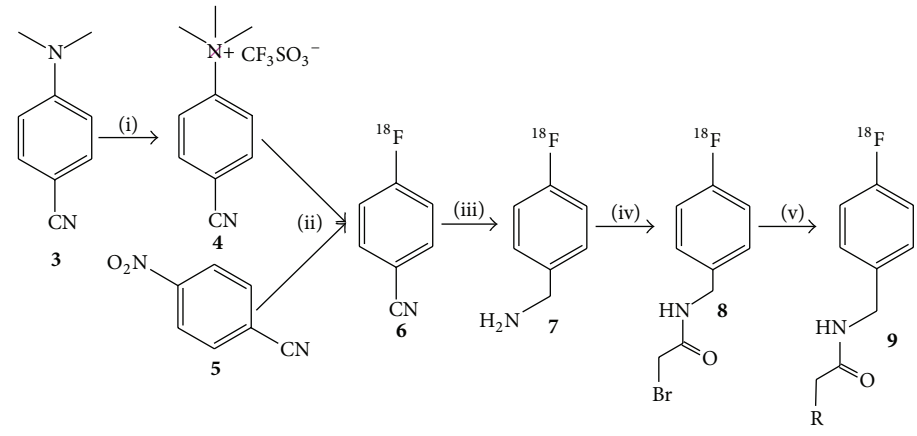

(a)

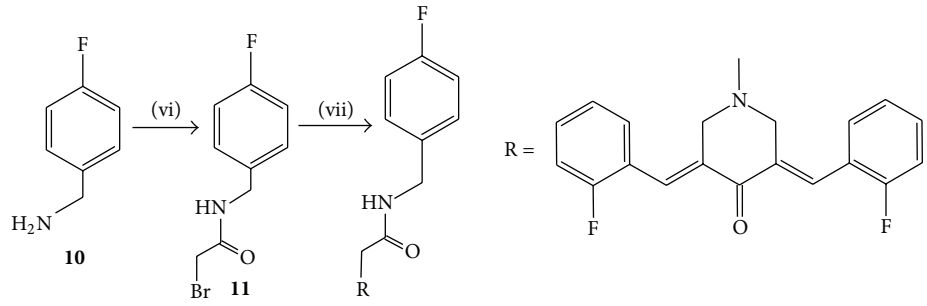

Authentic NFLOBA-EF24 (**12**)

(b)

Figure 2: Synthesis of ^{18}F-NFLOBA-EF24 (a) and authentic NFLOBA-EF24 (b). The reaction conditions were: (i) CF_3SO_3Me, benzene, 80°C, 1 h; (ii) [^{18}F]F^-, K(2.2.2), K_2CO_3, DMSO, 100°C, 15 min; (iii) 1 M $LiAlH_4$ in THF, 80°C, 5 min; (iv) bromoacetyl bromide, DCM, RT, 2 min; (v) EF24, Cs_2CO_3, KI, DMF, 85°C, 1 h; (vi) bromoacetyl bromide, triethylamine, DCM, RT, 2 h; (vii) EF24, Cs_2CO_3, KI, DMF, 85°C, 1 h.

acetonitrile gradient in water containing 0.1% TFA, over 15 min) at 254 nm wavelength. The radiochemical yield was approximately 60%.

*2.2.2. N-[4-Fluoro[^{18}F]-benzyl]-2-bromoacetamide (**8**).* $LiAlH_4$ solution in THF (1 mL of 1 M) was added to compound **6** in a reaction vial. The reaction was allowed to occur at 100°C for 5 min. After cooling to room temperature, the reaction mixture was diluted with 2 volumes of water, and 4-Fluoro[^{18}F]-benzylamine (**7**) was extracted into methylene chloride (5 mL). The organic phase was evaporated to reduce the volume by (1/5)th, before proceeding to the next step. Compound **7** showed a retention time of 9.9 min radio-UV-RPHPLC (5% to 100% acetonitrile gradient containing 0.1% TFA, over 15 min) at 254 nm wavelength. About 30 μL of 1 M solution of bromoacetyl bromide solution in methylene chloride was added to the concentrate of compound **7** from the previous step. The reaction mixture was warmed to 35°C for 5 min and filtered on a cotton plug with methylene chloride. The solvent was dried to obtain compound **8** that showed a retention time of 14.2 min in radio-UV-RPHPLC (5% to 100% acetonitrile containing 0.1% TFA, over 15 min) at 254 nm wavelength. Compound **8** was used as an ^{18}F-labeled synthon for conjugation with compound **2** in the next step.

*2.2.3. 2-[3,5-Bis-(2-fluorobenzylidene)-4-piperidon-1-yl]-N-[4-fluoro[^{18}F]-benzyl]acetamide (**9**).* Compound **8** was

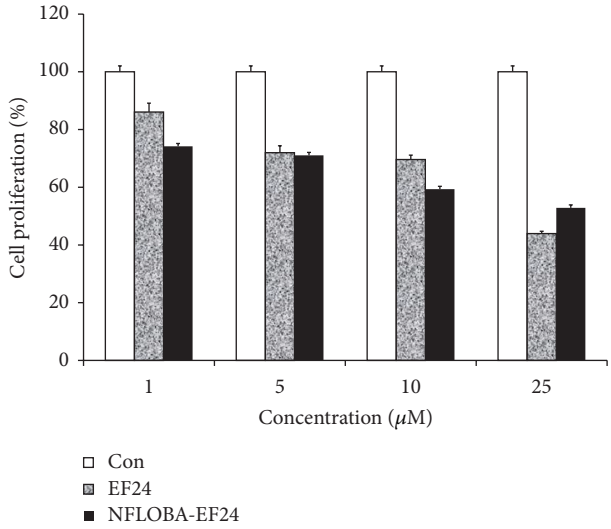

Figure 3: Cell proliferation assay using hexosaminidase assay. NFLOBA-EF24 derivative was compared with EF24 for inhibition of lung adenocarcinoma H441 cell proliferation.

dissolved in dimethylformamide or DMF (1 mL) and transferred to a reaction vial containing compound **2** (6.5 mg), KI (5 mg), and Cs_2CO_3 (6 mg). The reaction was allowed to occur at 100°C. After 40 min, the reaction mixture was filtered, and DMF was evaporated. On RP-HPLC, compound **9** had a retention time of 14.6 min (5% to 100% acetonitrile gradient containing 0.1% TFA, over 15 min) at 254 nm wavelength. Overall, the radiochemical yield was 40%.

2.3. Cell Culture and Drug Treatment. Human lung adenocarcinoma cell line NCI-H441 (ATCC Number: HTB-174) was obtained from American Type Culture Collection (Manassas, VA). H441 cells were maintained at 37°C with 5% CO_2 in McCoy's 5A Medium (Invitrogen, Carlsbad, California) supplemented with 5% heat-inactivated Fetal Bovine Serum (FBS) and Gentamicin (GIBCO Laboratories, Grand Island, NY). To evaluate the cytotoxicity of synthesized conjugate, H441 cells were seeded in a 96-well flat-bottom tissue culture plates at a density of 5×10^3 cells per well. The cells were allowed to attach and grow overnight. The test compound NFLOBA-EF24 was solubilized in dimethyl sulfoxide (DMSO) and added to cells at 5–25 μM concentration in McCoy's medium supplemented with 5% FBS. The DMSO concentration was maintained at 0.1% per well. Control wells received equivalent volume of DMSO without any drugs. The cells were allowed to remain in the treatment medium for 24 h.

2.3.1. Cell Proliferation. The total number of cells after 24 h of treatment was estimated by hexosaminidase assay [17]. Briefly, the medium was removed, and hexosaminidase substrate solution in citrate buffer pH 5 (7.5 mM), p-nitrophenol-*N*-acetyl-beta-D-glucosaminidase (Calbiochem, San Diego, CA), was added at 60 μL per well. The plate was incubated at 37°C in 100% humidity for 30 minutes, before stopping the reaction by adding 90 μL of 50 mM glycine containing 5 mM of EDTA (pH 10.4); absorbance was measured at 405 nm.

2.4. Animal Studies

2.4.1. PET Imaging and Biodistribution of ^{18}F-NFLOBA-EF24 in Normal Rats. The animal experiments were performed according to the NIH Animal Use and Care Guidelines and were approved by the Institutional Animal Care Committee of the University of Oklahoma Health Sciences Center. We investigated the distribution of ^{18}F-labeled compound **9** in normal Sprague Dawley rats ($n = 4$). PET imaging was performed in an X-PET machine (Gamma Medica-Ideas, Northridge, CA, USA). To reconcile the low solubility of F-18-labeled compound **9** in aqueous solvents, the injection formulation was prepared in 10% hydroxypropyl-β-cyclodextrin (HPβCD) in saline as described elsewhere [15]. Before injection, the solution was filtered through sterile 0.45 μm centrifugal filter.

For imaging, the rats were anesthetized using 2-3% isoflurane in oxygen stream and placed inside the PET detector. A fly-mode CT image was acquired to obtain anatomical landmarks and to enable appropriate positioning of the rats. The rats were repositioned inside the PET detector, and about 50 μCi of ^{18}F-labeled compound **9** (~0.2 mL) was intravenously injected in the tail vein. List-mode data was acquired for 1 h. PET images were reconstructed using filtered back projection algorithm and fused with the CT image. The fused image was used for analysis using Amira 3.1 software (Visage Image Inc., San Diego, CA, USA).

After the PET imaging, the rats were subjected to a biodistribution study. Briefly, the animals were euthanized by an intraperitoneal overdose of a euthanasia solution (Euthasol). Various organs were excised, washed with saline, and weighed, and appropriate tissue samples were counted in an automated gamma counter (Perkin-Elmer, Boston, MA). Total blood volume, bone, and muscle mass were estimated as 5.7%, 10%, and 40% of body weight, respectively, [18, 19]. A diluted sample of injected ^{18}F-labeled compound **9** served as a standard for comparison. The accumulation of injected preparation in various organs was also calculated as percent of injected radioactivity. All data were corrected for the decay of ^{18}F radioactivity (physical decay $T_{1/2} = 110$ min).

2.4.2. Therapeutic Treatment with NFLOBA-EF24 in Nude Rats with Xenograft Tumor. Female athymic nude rats (125–150 g) were obtained from Harlan Laboratories (Indianapolis, IN) and housed in a controlled environment with 12 h day/night cycle. The animals were allowed to acclimatize for at least 1 week before inoculation of lung adenocarcinoma H441 cells. On the day of tumor implantation, the animals were anesthetized with 2-3% isoflurane in oxygen stream. About 0.1 mL H441 cell suspension in phosphate-buffered saline (100 million cells/mL) was subcutaneously injected in the left dorsal thigh region. The animals were returned to their cages, and the tumor was allowed to grow till a palpable mass was visible in majority of the animals in about 7–10 days following implantation.

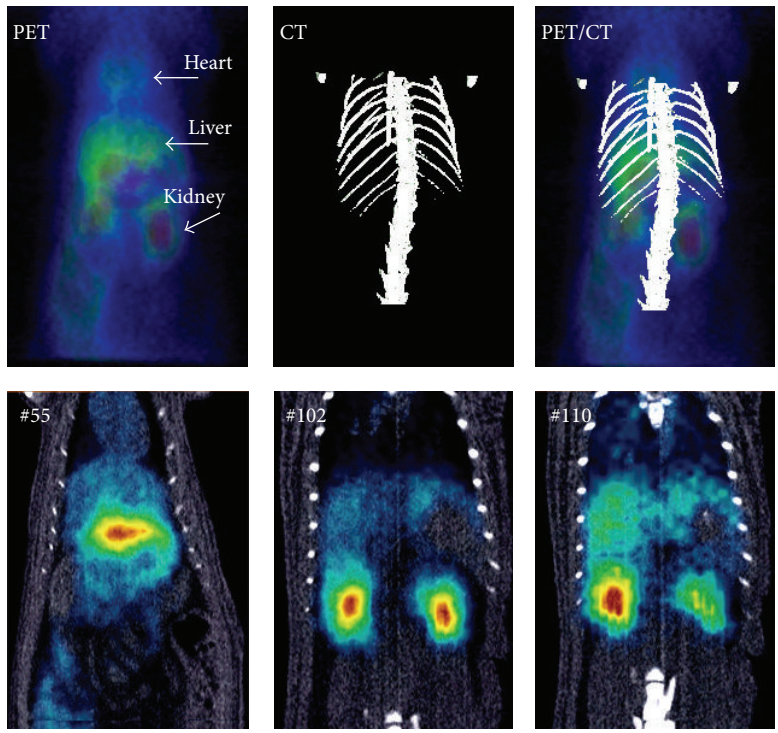

Figure 4: Representative PET images of a rat administered with ^{18}F-NFLOBA-EF24. Rats were intravenously injected with about 50 μCi of ^{18}F-NFLOBA-EF24 and imaged for 1 h. The composite data was fused with corresponding CT image and displayed in Amira 3.1 software. The upper panel shows the volume-rendered images, whereas the lower panel shows selected coronal slices (nos. 55, 102, and 110) for better visualization of hepatic and renal accumulation.

The treatment was started on day 8 of tumor implantation. Nonradioactive NFLOBA-EF24 (**12**) in DMSO solution was intraperitoneally injected every second day at a dose of 400 μg/Kg. The treatment was continued for 15 days.

2.4.3. Monitoring of Tumor Suppressive Effect. On each injection day the tumor growth was determined by measuring two dimensions using the Vernier calipers to obtain tumor volume = (Length × Width^2)/2. Finally, the percent of tumor growth inhibition treatment was determined by using the following formula: % tumor growth inhibition = $[(1 - T/C) * 100]$, where T and C are mean tumor volumes in the treated and control groups, respectively.

On the 16th day, a select group of animals ($n = 3$ each for control and treated) were subjected to PET imaging using ^{18}F-fluorodeoxyglucose (^{18}F-FDG). Briefly, the rats were prepared for PET imaging as described above. About 75 μCi of ^{18}F-FDG was intravenously administered and allowed to distribute for 2 h. After two hours, the rats were anesthetized again for PET imaging. A static image of lower body field-of-view was acquired for 15 min. An accompanying CT image was used to anatomically localize ^{18}F-FDG accumulation. The images were reconstructed as described above.

2.5. Data Analysis. The *in vitro* biological data was analyzed for significance of difference at $P < 0.05$ using Prism 5.0 (GraphPad Software, Inc., La Jolla, CA). The *in vivo* biodistribution data was calculated for presentation as percent of injected dose per gram tissue as well as per organ. The PET and CT image fusion and further image manipulations were carried out using scripts written in the Amira 3.1.1 software (Visage Imaging, Inc., San Diego, CA).

3. Results

In the chemical modification reported in this work, a known synthetic curcuminoid 3,5-bis-(2-fluorobenzylidene)-4-piperidone (EF24, **2**) is the base compound. The objective was to enable real-time biodisposition studies of EF24. The modification is characterized by an ability to introduce imageable ^{18}F radionuclide in the molecule. We compared the antiproliferative activity of the modified imageable analog against EF24 and provided a glimpse of its *in vivo* distribution by PET imaging. We and others have also shown that most *N*-modifications preserved the antiproliferative activity of EF24 [8, 20–22].

*3.1. 2-[3,5-Bis-(2-fluorobenzylidene)-4-piperidon-1-yl]-N-[4-fluoro[^{18}F]-benzyl]acetamide (**9**).* To enable ^{18}F labeling of EF24, we synthesized a highly reactive ^{18}F-labeled synthon **8** (NFLOBA) via a multistep approach. We first synthesized 4-fluoro (^{18}F)-benzonitrile (**6**) as an ^{18}F-labeled intermediate. Compound **6** was synthesized by a kryptofix-mediated nucleophilic displacement in 4-cyano-*N*,*N*,*N*-trimethylanilinium trifluoromethanesulfonate **4** (Figure 2(a)). Radiochemical yield of over 60% was obtained.

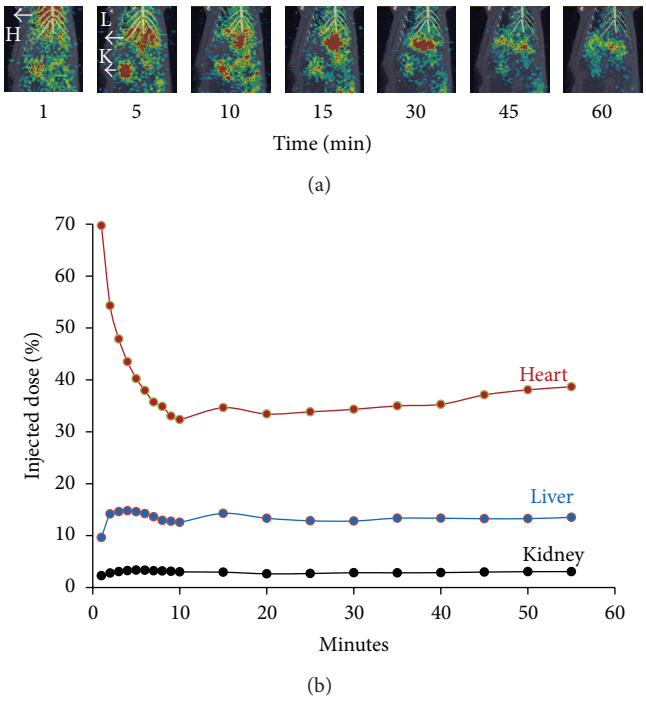

Figure 5: The dynamic clearance data obtained by drawing regions of interest around heart, liver, and kidney in reconstructed PET images. Heart-bound radioactivity may be partially indicative of NFLOBA-EF24 circulating in blood. The time-specific PET images in inset (a) show visual clearance of labeled drug from the body with respect to time.

The chemical identity of compound **6** was confirmed by coelution with reference standard 4-fluorobenzonitrile in reverse phase HPLC (C-18, Sonoma column, 5% to 100% acetonitrile gradient containing 0.1% TFA, over 15 min). In an alternative synthetic scheme, 4-fluoro[^{18}F]-benzonitrile was also obtained from a 4-nitrobenzonitrile precursor (**5**) in 50% RCY (Figure 2(a)). Because of smaller yields and difficult work-up, we abandoned this alternative scheme and utilized labeling reactions using precursor **4**.

Reduction of 4-fluoro[^{18}F]-benzonitrile (**6**) with $LiAlH_4$ afforded 4-fluoro[^{18}F]-benzylamine (**7**) in quantitative yields. Further reaction of compound **7** with bromoacetyl bromide provided *N*-(4-fluorobenzyl)-2-bromoacetamide **8** (NFLOBA) which upon reaction with compound **2** resulted in 2-[3,5-bis(2-fluorobenzylidene-4-piperidon-1-yl)-*N*-4-fluoro[^{18}F]-benzyl] acetamide] (**9**) in good yields (40–45% decay-corrected radiochemical yield). Compound **9** was designated as NFLOBA-EF24. The elution characteristics of ^{18}F-labeled NFLOBA-EF24 were compared with nonradioactive authentic NFLOBA-EF24 on reverse-phase HPLC. NFLOBA-EF24 showed a retention time of 14.6 min (Supplemental Material). All the intermediate radioactive compounds (**6**, **7**, and **8**) were also monitored with radio/UV-reverse phase HPLC and compared with their respective standards. The synthesis of the authentic nonradioactive NFLOBA-EF24 is provided in (Figure 2(b)).

3.2. In Vitro Anticancer Activity of NFLOBA-EF24. Since the radiolabeled compounds are chemically modified to enable radiolabeling, we investigated if the cold analog NFLOBA-EF24 retained the antiproliferative activity associated with EF24 in lung adenocarcinoma H441 cells. Form the data in Figure 3, it is clear that NFLOBA modification did not affect the proliferation-suppressive activity of EF24. Any apparent difference between the precursor EF24 and NFLOBA-EF24 was not statistically significant. Therefore, we pursued *in vivo* testing of the radiolabeled analog of NFLOBA-EF24.

3.3. PET Imaging and Biodistribution. Radiolabeled ^{18}F-NFLOBA-EF24 was investigated in normal rats by PET imaging and biodistribution at necropsy. CT provided anatomical landmarks for easy identification and localization of radioactivity in various organs. As shown in the fused PET/CT images (Figure 4), ^{18}F-NFLOBA-EF24 distributed in various organs of the body. The major organs of uptake appeared to be liver and kidney with moderate amounts circulating in blood. To study the kinetics of accumulation in liver and kidney, the list-mode image data was fragmented into twelve segments—each of 5 min duration, and time-activity plots were generated (Figure 5). The corresponding images are shown in the inset (Figure 5(a)). The rapid decline in radioactivity in the blood pool was accompanied by a corresponding increase in accumulation in organs responsible for clearance, namely, liver and kidney. The levels in blood, kidney, and liver appeared to plateau within 10 min of administration. We collected rat urine after 1 h of injection and analyzed it by radio-HPLC; a single peak corresponding to the intact NFLOBA-EF24 was observed, suggesting that the injected analog was cleared by kidney unmodified.

The biodistribution data of ^{18}F-NFLOBA-EF24 after necropsy at 1 h is shown in Figure 6. Kidney, liver, and muscle were the tissues of significant accumulation. There was negligible association of radioactivity with the bone tissue, suggesting that the radiolabeled compound was stable, and no *in vivo* defluorination occurred. The total radioactivity recovered in the major organs was approximately 40%. We conjecture that the rest of the injected dose was excreted in the urine. Because of the experimental setting, we could not quantitatively recover urine, but the radioactivity counts in the fractional urine collected always exceeded any other organ counts.

3.4. NFLOBA-EF24 Suppresses Tumor Growth. In order to investigate the retention of tumor-suppressive characteristic of EF24 *in vivo*, we tested NFLOBA-EF24 in nude rats implanted with H441 tumor. Administration of NFLOBA-EF24 every second day reduced the tumor growth in the treated rats as compared to the control rats receiving equal amounts of vehicle (Figure 7(a)). Since the rats were randomized without any regard to tumor volume, the initial tumor volume (Day 1) between the treated and control groups was not significant. With each progressive NFLOBA-EF24 injection, the tumor size decreased; in 2/6 rats the tumor became unpalpable by the 15th day. Based on average tumor size, the percent of tumor inhibition as of day 15 of treatment

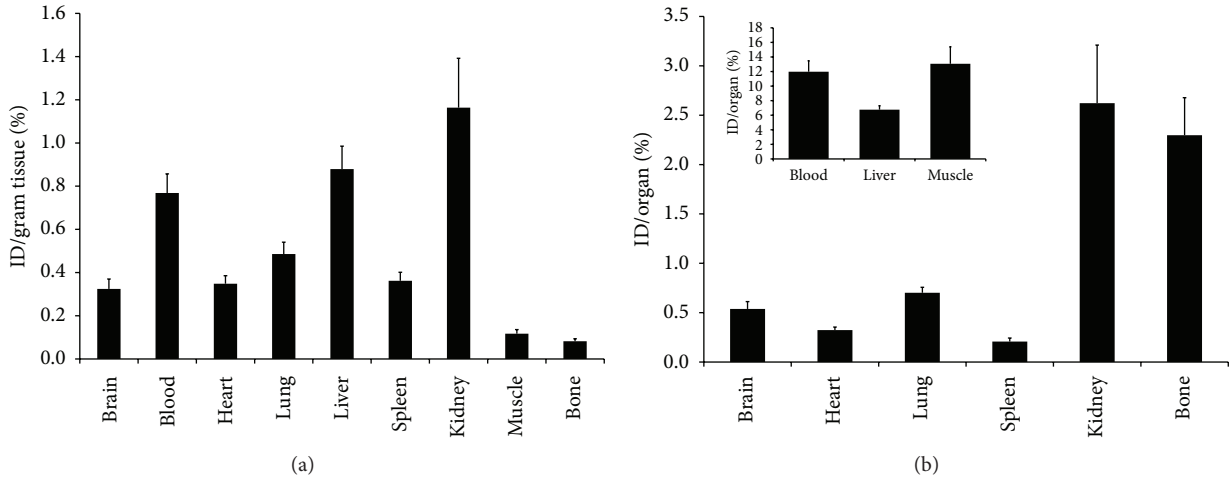

FIGURE 6: Biodistribution of ^{18}F-NFLOBA-EF24 in normal Sprague Dawley rats ($n = 4$). The data has been presented as (a) percent of injected dose per gram tissue and (b) percent of injected dose accumulated in whole organ.

was calculated to be approximately 83%. To demonstrate the efficacy of NFLOBA-EF24 by molecular imaging of glucose uptake, we performed ^{18}F-FDG-PET imaging in randomly selected three rats from control and treated groups. The magnitude of ^{18}F-FDG uptake is indicative of tissue glucose metabolism, which is expected to be higher in growing tumor. It is clear from the representative images that NFLOBA-EF24 indeed decreased ^{18}F-FDG uptake in tumor tissue (Figure 7(b)).

4. Discussion

Despite recent advances in molecular understanding of tumor biology and the introduction of several new therapeutic agents, cancer continues to have an overall dismal survival. Chemotherapy, together with radiation therapy, and surgery are the alternatives available for the treatment of cancer. Since antineoplastic agents are cytotoxic by design and can cause severe systemic adverse effects in therapeutic doses, it is vital to gather information about drug's biodisposition after administration. This approach is based on the drug development philosophy that it is not only necessary to develop a new therapeutic molecule, but it is also important to noninvasively assay accumulation of the molecule in the intended tissue or organ. Whole-body imaging is one approach to monitor drug kinetics on real-time basis, provided the drug could be tagged with a moiety detectable by external detectors. PET offers an option by virtue of its high resolution, high sensitivity, and the recent progress made in the radiochemistry involving positron-emitting ^{18}F and ^{11}C radionuclides. Whereas ^{11}C is a natural replacement for carbon atoms in a drug and does not alter the structure of the drug, ^{18}F radiochemistry often results in a molecule significantly different from the active drug. Unfortunately, short decay half-life of ^{11}C (20 min) and the requirement of the access to a nearby cyclotron prohibit many researchers from indulging in ^{11}C radiochemical synthesis. On the other hand, ^{18}F offers relatively more time (decay half-life 110 min) to perform multistep synthesis. Therefore, we chose ^{18}F for radiolabeling and imaging of EF24.

Curcumin and its synthetic analogs have shown some specificity in regards to being antiproliferative in cancerous cells without being toxic to normal cells [23]. Like curcumin, EF24 possesses conjugated enone moiety. It has been proposed that conjugated enones inhibit glutathione-*S*-transferase which enhances the cytotoxicity of these compounds [24]. The enone moiety present in this class of compounds permits addition of thiol groups in intracellular compounds, such as glutathione, to the olefinic double bond. The addition product is capable of further reacting with cellular nucleophiles and consequently contributes to the observed cytotoxicity [6, 25]. We hypothesized that since enone group in EF24 is structurally away from piperidonyl N-atom, relatively modest N-substitution would not alter the biochemical basis of EF24's action. Indeed, we found a series of 3,5-bis-benzylidene-4-piperidone compounds to be very effective in inhibiting cell proliferation of lung adenocarcinoma cells, and N-substitution with relatively small moieties does not significantly affect the anticancer activity of lead compound EF24 [22]. On this basis we further hypothesized that the piperidonyl nitrogen of EF24 could be similarly modified to carry PET imageable radionuclide ^{18}F.

In this study, we modified EF24 to carry an ^{18}F-labeled synthon at the piperidonyl nitrogen. Because of the short decay half-life, the radiochemical schemes involving ^{18}F are necessarily required to be efficient and quick. We accomplished the reactions of modifying EF24 with NFLOBA within a reasonable time period of 2.5 h per reaction. At the same time, the chemical modifications should not interfere with the intended biological activity of the compound. Using nonradioactive authentic NFLOBA-EF24, we established that it retained *in vitro* antiproliferative potency of EF24. However, the modification might have substantially altered the physicochemical properties. For instance, the partition coefficient of NFLOBA-EF24 ($\log P = 2.36$) exceeds that of EF24

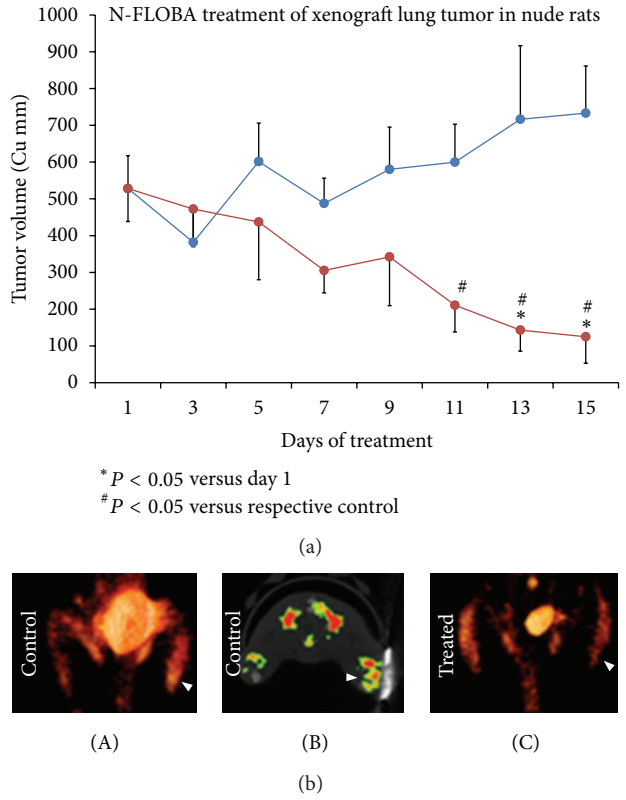

Figure 7: (a) Changes in xenograft tumor volume with respect to the treatment either with NFLOBA-EF24 (treated) or with vehicle (control). (b) Representative PET images of F-18-FDG accumulation in tumor tissue of a control (A and B) and a treated rat (C). Picture (A) and (C) are volume-rendered images, whereas picture (B) is an axial view. Tumor was localized by fusion of PET images with CT images. The CT image of tumor tissue was accentuated by pasting an X-ray opaque tape on the tumor skin.

($\log P = 0.45$) by several folds. Although such changes may have a significant impact on the overall *in vivo* behavior of the modified drug, NFLOBA-EF24 still passes one of the drug-likeness test of Lipinski's which states that drugs with $\log P < 5.0$ are likely to be candidates for bioavailability from the oral route of administration [26]. Nonetheless, the low aqueous solubility of NFLOBA-EF24 was prohibitive in making an intravenous injection of radiolabeled compound. Therefore, we followed a strategy of using an inclusion complex of ^{18}F-NFLOBA-EF24 for enabling parenteral administration. We have characterized such complexes to show that HPβCD can serve as a host to the guest compounds, such as EF24 [15, 27]. Many successful drug formulations in the market are based on solubilizing drugs as cyclodextrin inclusion complexes [28]. It has been shown by others that cyclodextrin inclusion complexes are subject to rapid excretion in urine [29].

The PET images of ^{18}F-NFLOBA-EF24 in normal rats demonstrated that it widely distributes in the body. The absence of radioactivity accumulation in bone tissue suggested that no metabolic defluorination occurred *in vivo*. Approximately 70% of injected dose was cleared from blood within 10 min of injection (Figure 5). Evidently, liver and kidney were responsible for the rapid clearance of NFLOBA-EF24. The accumulation of NFLOBA-EF24 in kidney and liver stabilized and almost plateaued after 10–15 min after injection. The postimaging biodistribution data confirmed the image-derived information. The uptake in muscle was perhaps indicative of the blood borne radioactivity because of the highly vascular nature of the muscle tissue.

In most circumstances, the chemical modifications for fluorescent- or radio-tagging of drugs results in a significant compromise of efficacy. Our *in vitro* data on cell proliferation demonstrated that the NFLOBA modification of EF24 does not seem to adversely influence the efficacy of the drug. NFLOBA-EF24 was also found effective *in vivo*, as was evident by the reduction in the growth of tumor in treated animals. Since, the tumor volume measurements may be confounding at times because of the inflammation secondary to necrosis, we confirmed our findings by PET imaging of ^{18}F-FDG accumulation in tumor. There was a difference in uptake of ^{18}F-FDG in tumor tissue of treated and control rats (Figure 7(b)).

In summary, we report the synthesis of NFLOBA-EF24 which could provide a platform for application of imaging technologies in the development of more potent EF24 derivatives. Anticancer therapy combined with image-derived knowledge of drug accumulation enables a more realistic and effective treatment planning and may be of benefit in predicating the tumor response as well as in enabling timely change of course, in case of poor image signal from the tumor.

Disclosure

The authors do not have any direct financial interests to disclose in relation to the research reported in this article.

Acknowledgments

The authors are thankful to OUHSC College of Pharmacy (for a seed grant to Pallavi Lagisetty), and acknowledge the funding from National Cancer Institute (R03 CA143614-01 to Vibhudutta Awasthi). Technical help from Sandra Bryant (OUHSC, Oklahoma City) and Mr. Kaustuv Sahoo (Graduate Student) is also acknowledged.

References

[1] G. L. Griffiths, "The imaging probe development center and the production of molecular imaging probes," *Current Chemical Genomics*, vol. 1, pp. 65–69, 2008.

[2] M. G. Pomper, "Can small animal imaging accelerate drug development?" *Journal of Cellular Biochemistry*, no. 39, pp. 211–220, 2002.

[3] C. A. Altar, "The biomarkers consortium: on the critical path of drug discovery," *Clinical Pharmacology and Therapeutics*, vol. 83, no. 2, pp. 361–364, 2008.

[4] C. A. Altar, D. Amakye, D. Bounos et al., "A prototypical process for creating evidentiary standards for biomarkers and diagnostics," *Clinical Pharmacology and Therapeutics*, vol. 83, no. 2, pp. 368–371, 2008.

[5] J. Woodcock and R. Woosley, "The FDA critical path initiative and its influence on new drug development," *Annual Review of Medicine*, vol. 59, pp. 1–12, 2008.

[6] A. Iagaru, S. S. Gambhir, and M. L. Goris, "90Y-ibritumomab therapy in refractory non-Hodgkin's lymphoma: observations from 111In-ibritumomab pretreatment imaging," *Journal of Nuclear Medicine*, vol. 49, no. 11, pp. 1809–1812, 2008.

[7] P. Anand, A. B. Kunnumakkara, R. A. Newman, and B. B. Aggarwal, "Bioavailability of curcumin: problems and promises," *Molecular Pharmaceutics*, vol. 4, no. 6, pp. 807–818, 2007.

[8] H. N. Pati, U. Das, J. W. Quail, M. Kawase, H. Sakagami, and J. R. Dimmock, "Cytotoxic 3,5-bis(benzylidene)piperidin-4-ones and N-acyl analogs displaying selective toxicity for malignant cells," *European Journal of Medicinal Chemistry*, vol. 43, no. 1, pp. 1–7, 2008.

[9] T. P. Robinson, R. B. Hubbard, T. J. Ehlers, J. L. Arbiser, D. J. Goldsmith, and J. P. Bowen, "Synthesis and biological evaluation of aromatic enones related to curcumin," *Bioorganic and Medicinal Chemistry*, vol. 13, no. 12, pp. 4007–4013, 2005.

[10] A. Sun, M. Shoji, Y. J. Lu, D. C. Liotta, and J. P. Snyder, "Synthesis of EF24-tripeptide chloromethyl ketone: a novel curcumin-related anticancer drug delivery system," *Journal of Medicinal Chemistry*, vol. 49, no. 11, pp. 3153–3158, 2006.

[11] D. Subramaniam, R. May, S. M. Sureban et al., "Diphenyl difluoroketone: a curcumin derivative with potent in vivo anticancer activity," *Cancer Research*, vol. 68, no. 6, pp. 1962–1969, 2008.

[12] K. Selvendiran, L. Tong, S. Vishwanath et al., "EF24 induces G2/M arrest and apoptosis in cisplatin-resistant human ovarian cancer cells by increasing PTEN expression," *Journal of Biological Chemistry*, vol. 282, no. 39, pp. 28609–28618, 2007.

[13] B. K. Adams, E. M. Ferstl, M. C. Davis et al., "Synthesis and biological evaluation of novel curcumin analogs as anti-cancer and anti-angiogenesis agents," *Bioorganic and Medicinal Chemistry*, vol. 12, no. 14, pp. 3871–3883, 2004.

[14] A. L. Kasinski, Y. Du, S. L. Thomas et al., "Inhibition of IκB kinase-nuclear factor-κB signaling pathway by 3,5-bis(2-flurobenzylidene)piperidin-4-one (EF24), a novel monoketone analog of curcumin?" *Molecular Pharmacology*, vol. 74, no. 3, pp. 654–661, 2008.

[15] H. Agashe, K. Sahoo, P. Lagisetty, and V. Awasthi, "Cyclodextrin-mediated entrapment of curcuminoid 4-[3,5-bis(2-chlorobenzylidene-4-oxo-piperidine-1-yl)-4-oxo-2-butenoic acid] or CLEFMA in liposomes for treatment of xenograft lung tumor in rats," *Colloids and Surfaces B*, vol. 84, no. 2, pp. 329–337, 2011.

[16] P. Lagisetty, D. R. Powell, and V. Awasthi, "Synthesis and structural determination of 3,5-bis(2-fluorobenzylidene)-4-piperidone analogs of curcumin," *Journal of Molecular Structure*, vol. 936, no. 1–3, pp. 23–28, 2009.

[17] U. Landegren, "Measurement of cell numbers by means of the endogenous enzyme hexosaminidase. Applications to detection of lymphokines and cell surface antigens," *Journal of Immunological Methods*, vol. 67, no. 2, pp. 379–388, 1984.

[18] D. W. Frank, "Physiological data of laboratory animals," in *Handbook of Laboratory Animal Science*, E. C. Melby Jr., Ed., vol. 3, pp. 23–64, CRC Press, Boca Raton, Fla, USA, 1976.

[19] C. Petty, *Research Techniques in the Rats*, Charles C. Thomas, Springfield, Ill, USA, 1982.

[20] U. Das, S. Das, B. Bandy, J. P. Stables, and J. R. Dimmock, "N-Aroyl-3,5-bis(benzylidene)-4-piperidones: a novel class of antimycobacterial agents," *Bioorganic and Medicinal Chemistry*, vol. 16, no. 7, pp. 3602–3607, 2008.

[21] E. K. Ryu, Y. S. Choe, K.-H. Lee, Y. Choi, and B.-T. Kim, "Curcumin and dehydrozingerone derivatives: synthesis, radiolabeling, and evaluation for β-amyloid plaque imaging," *Journal of Medicinal Chemistry*, vol. 49, no. 20, pp. 6111–6119, 2006.

[22] P. Lagisetty, P. Vilekar, K. Sahoo, S. Anant, and V. Awasthi, "CLEFMA—an anti-proliferative curcuminoid from structure-activity relationship studies on 3,5-bis(benzylidene)-4-piperidones," *Bioorganic and Medicinal Chemistry*, vol. 18, no. 16, pp. 6109–6120, 2010.

[23] J. Ravindran, S. Prasad, and B. B. Aggarwal, "Curcumin and cancer cells: how many ways can curry kill tumor cells selectively?" *AAPS Journal*, vol. 11, no. 3, pp. 495–510, 2009.

[24] P. J. O'Dwyer, F. LaCreta, S. Nash et al., "Phase I study of thiotepa in combination with the glutathione transferase inhibitor ethacrynic acid," *Cancer Research*, vol. 51, no. 22, pp. 6059–6065, 1991.

[25] R. Costi, R. Di Santo, M. Artico et al., "2,6-Bis(3,4,5-trihydroxybenzylydene) derivatives of cyclohexanone: novel potent HIV-1 integrase inhibitors that prevent HIV-1 multiplication in cell-based assays," *Bioorganic and Medicinal Chemistry*, vol. 12, no. 1, pp. 199–215, 2004.

[26] C. A. Lipinski, F. Lombardo, B. W. Dominy, and P. J. Feeney, "Experimental and computational approaches to estimate solubility and permeability in drug discovery and development settings," *Advanced Drug Delivery Reviews*, vol. 46, no. 1–3, pp. 3–26, 2001.

[27] H. Agashe, P. Lagisetty, K. Sahoo, D. Bourne, B. Grady, and V. Awasthi, "Liposome-encapsulated EF24-HPβCD inclusion complex: a preformulation study and biodistribution in a rat model," *Journal of Nanoparticle Research*, vol. 13, no. 6, pp. 2609–2623, 2011.

[28] V. J. Stella and Q. He, "Cyclodextrins," *Toxicologic Pathology*, vol. 36, pp. 30–42, 2008.

[29] V. J. Stella, V. M. Rao, E. A. Zannou, and V. Zia, "Mechanisms of drug release from cyclodextrin complexes," *Advanced Drug Delivery Reviews*, vol. 36, no. 1, pp. 3–16, 1999.